Detection of CO_2 leakage from a simulated sub-seabed storage site using three different types of pCO_2 sensors

Dariia Atamanchuk[1,*], Anders Tengberg[1,2], Dmitry Aleynik[3], Peer Fietzek[4], Kiminori Shitashima[5], Anna Lichtschlag[6], Per O.J. Hall[1], Henrik Stahl[3]

[1]Department of Chemistry and Molecular Biology, Marine Chemistry, University of Gothenburg, SE-41296 Gothenburg, Sweden

[2]Aanderaa Data Instruments AS, Midtun, NO-5828 Bergen, Norway

[3]Scottish Association for Marine Science, Scottish Marine Institute, Oban, Argyll, PA37 1QA, UK

[4]GEOMAR Helmholtz Centre for Ocean Research, 24148 Kiel, Germany and CONTROS Systems & Solutions GmbH, 24148 Kiel, Germany

[5]International Institute for Carbon-Neutral Energy Research, Kyushu University, Kasuga-Kouen, 816-8580 Fukuoka, Japan

[6]National Oceanography Centre, University of Southampton Waterfront Campus, European Way, Southampton, SO14 3ZH, UK

[*]*Corresponding author*

dariia@chem.gu.se

Tel: +46-31-786-9063

Abstract

This work is focused on results from a recent controlled sub-seabed in situ carbon dioxide (CO_2) release experiment (QICS: Quantifying and Monitoring Potential Ecosystem Impacts of Geological Carbon Storage) carried out during May-October 2012 in Ardmucknish Bay on the Scottish west coast. Three types of pCO_2 sensors (fluorescence, NDIR and ISFET-based technologies) were used in combination with multiparameter instruments measuring oxygen, temperature, salinity and currents in the water column at the epicentre of release and further away. It was shown that distribution of seafloor CO_2 emissions features high spatial and temporal heterogeneity. The highest pCO_2 values (~1250 µatm) were detected at low tide around a bubble stream and within centimetres distance from the seafloor. Further up in the water column, 30 to 100 cm above the seabed, the gradients decreased, but continued to indicate elevated pCO_2 at the epicentre of release throughout the injection campaign with the peak values between 400 and 740 µatm. High-frequency parallel measurements from two instruments placed within 1 m from each other, relocation of one of the instruments at the release site and 2D horizontal mapping of the release and control sites confirmed a localized impact from CO_2 emissions. Observed effects on the water column were temporary and post-injection recovery took <7 days.

A multivariate statistical approach was used to recognize the periods when the system was dominated by natural forcing with strong correlation between variation in pCO_2 and O_2, and when it was influenced by purposefully released CO_2.

Use of a hydrodynamic circulation model, calibrated with in situ data, was crucial to establishing background conditions in this complex and dynamic shallow water system.

1. **Introduction**

Carbon Capture and Storage (CCS) is a method of capturing CO_2 from large point emitters, such as fossil fuel based power plants and heavy industry, and its sequestration into geological storage sites, e.g. deep geological formation covered by sealing caprock. This approach has been suggested as a potentially significant mitigation strategy to counteract climate change and ocean acidification (Gough and Shackley, 2005; Haszeldine, 2009; Wilkinson et al., 2013).

Before sub-sea CO_2 storage can be carried out on a commercial scale, ecological consequences as well as adverse environmental and human impacts of potential CO_2 leakages need to be identified and reliable monitoring strategies for detection and quantification of potential leakages, both acute (broken pipes, leaking connections, etc.) and chronic (faults in the geological caprock), need to be developed.

Previous efforts to study controlled CO_2 releases with the focus on environmental impact and detectability were restricted by either small-scale direct injections of liquid CO_2 into the deep water layers or model studies of the fate of released CO_2. Small-scale liquid CO_2 injections were carried out in a series of experiments off the coast of California (Brewer et al., 2003, 2004), which later developed into the FOCE (Free Ocean CO_2 Enrichment) program (Kirkwood et al., 2005, 2009; Walz et al., 2008).

Modelling studies based on natural CO_2 releases in Kagoshima Bay described physico-chemical processes of CO_2 transformation in seawater (Dissanayke et al., 2012). Numerous models were developed to predict the behaviour of leaking CO_2, purposefully stored under the seabed (Blackford et al., 2008; Kano et al., 2010; Dewar et al., 2013), and as a consequence the rise of pCO_2 (Kano et al., 2009) or the transformation pathways of released CO_2 in the deep ocean (Jeong et al., 2010).

Natural marine CO_2 seepage sites, like the one off the coast of Panarea Island, Southern Italy, are widely and extensively studied in terms of assessment of CO_2 impacts to seawater chemistry and ecology (Pearce et al., 2014).

Within the NERC funded research project QICS (Quantifying and Monitoring Potential Ecosystem Impacts of Geological Carbon Storage) a large scale controlled *in situ* CO_2 sub-seabed release was conducted in Ardmucknish Bay, Scotland (Fig. 1) in spring-summer of 2012, in order to make a realistic simulation of CO_2 leakage event. An overview of the physical aspects of CO_2 migration through the sediment overburden and overlying water column, as well as of the ecological and biogeochemical impacts on the benthos, of this experiment were recently described in Blackford et al. (submitted).

This paper focuses on challenges and technical aspects of detecting CO_2 emissions in the overlying water from this shallow water release experiment, using three different types of pCO_2 sensors in combination with standard hydrographical instrumentation for additional properties of seawater.

In this study we address the following questions:

How much did the CO_2 release affect the pCO_2 in the water column at different distances from the source and how did it compare to background natural variability? What was the spatial and temporal heterogeneity of the CO_2 plume in the water column during the release, and how quick was the recovery after the termination of the release? What parameters need to be measured in order to explain and model the changes in the carbonate system caused by CO_2 release? Which technical solutions for monitoring systems at storage sites, fixed and movable, would allow detection and/or identification CO_2 leakages with the highest probability?

2. Materials and methods

2.1. Study site and CO_2 release experiment

The CO_2 release experiment (QICS) was carried out in Ardmucknish Bay, near Oban on the Scottish west coast (Fig. 1, *inset*). After identification of a suitable site in the vicinity of the Scottish Association for Marine Science (SAMS, Dunstaffnage, Oban) (Taylor et al., this volume), a thorough baseline survey was conducted during autumn of 2011 and in early 2012. The latter included a combination of acoustic surveys, sediment coring and diver-based characterization of background conditions prior to drilling and injection of CO_2.

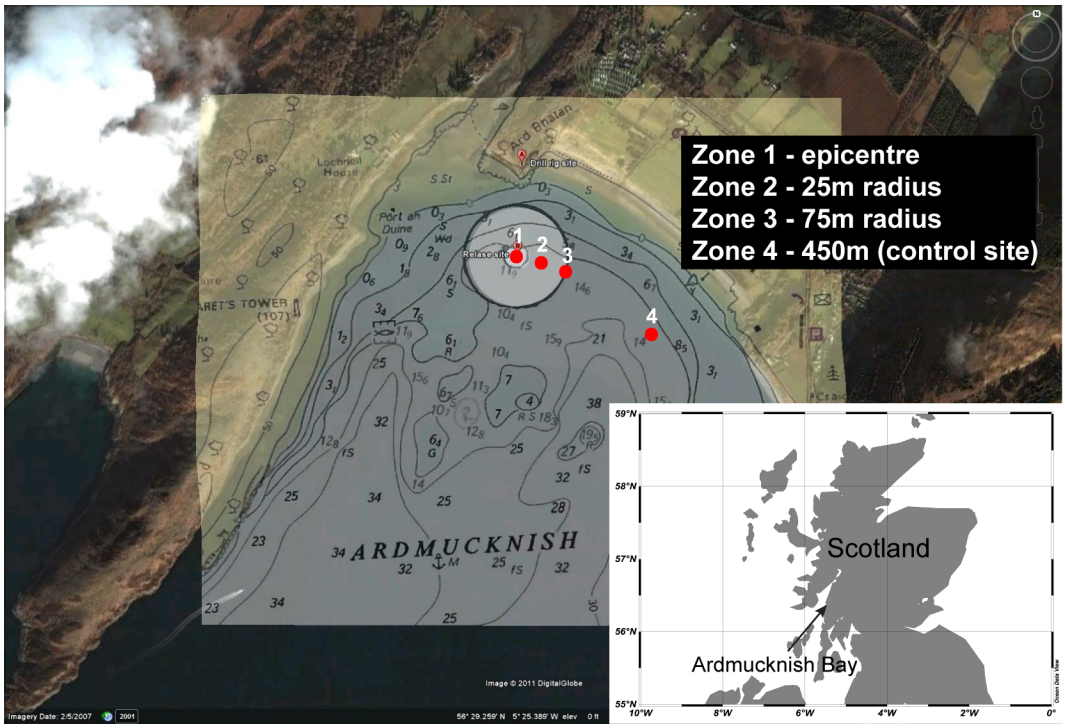

Fig. 1. Satellite picture of Ardmucknish Bay (https://maps.google.com) where the release of CO_2 gas took place with indication of sampling sites (red circles) at Zones 1-4. *Inset:* The study site Ardmucknish Bay, Oban, Scotland on the map.

In the beginning of 2012 (February-April), a southerly facing borehole was drilled, using a directional drilling rig, through the bedrock and terminating 10 m

horizontally into unconsolidated sediments 350 m offshore in the northern part of the bay (Fig. 2a; see also https://www.youtube.com/watch?v=bhmCGcEenjk and Supplementary material).

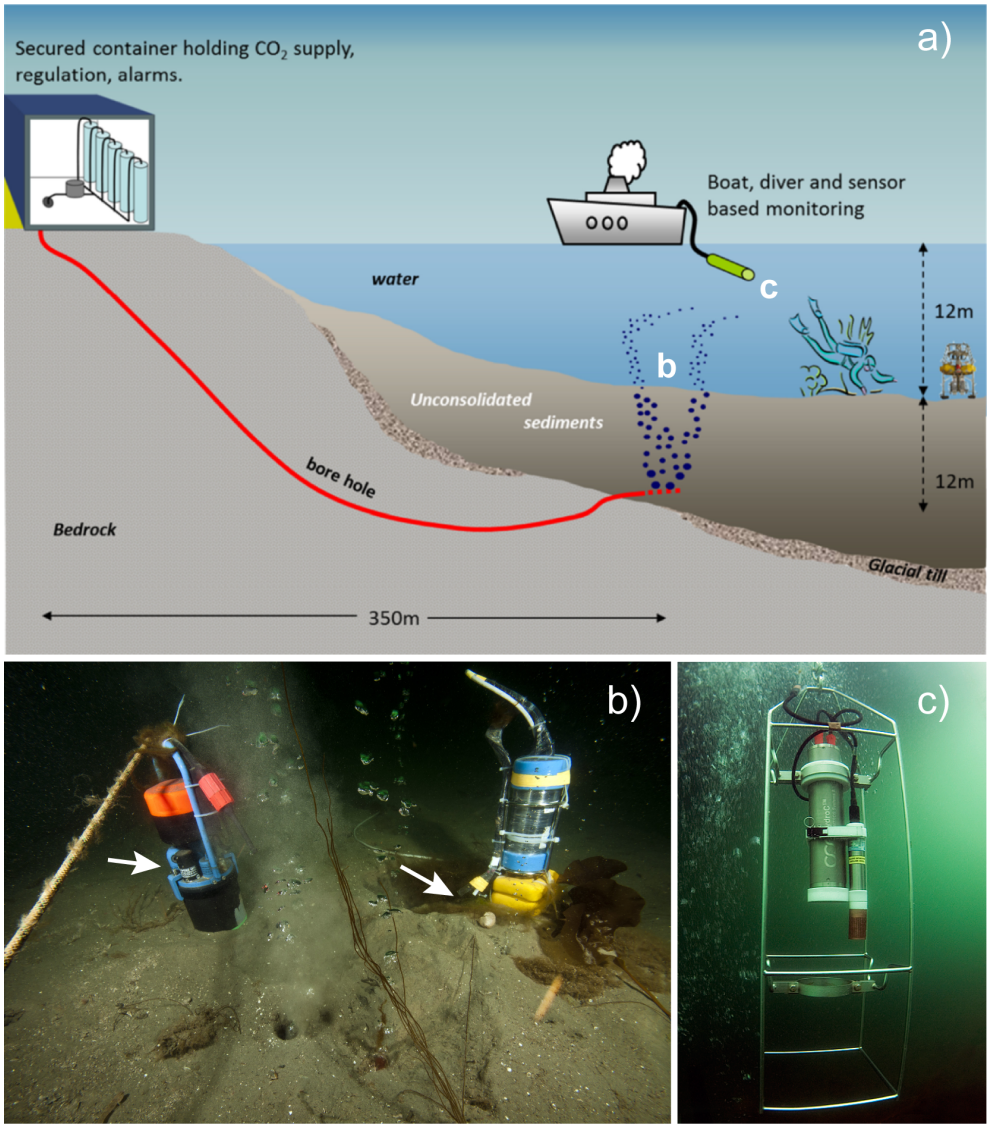

Fig. 2. a) Schematic of the QICS *in situ* release experiment indicating the relative locations (b and c) of the pCO_2 sensors used in this study; b) Photo of Seaguard® (left) and ISFET (right) pCO_2 sensors deployed *in situ* next to CO_2 bubble streams. White arrows indicate positions of sensors on the instruments, 30 and 3 cm above the bottom, respectively; c) Underwater photo of the towed CONTROS HydroC™ pCO_2 sensor.

The CO_2 gas was released from a land-based container, through a 20 mm diameter welded stainless steel pipeline terminating in a 5 m long diffuser with multiple 0.5 mm perforations located 11 m below the seabed. The overlying water depth at the

study site was 10-12 m depending on the tide. The injection phase started on May 17th and lasted for 37 days (day 0 to 36) until June 22nd, followed by the recovery period, until November 1st. CO_2 injection rates commenced at 10 kg CO_2 d^{-1} at day 0, increasing to 83 kg CO_2 d^{-1} by day 3, 150 kg CO_2 d^{-1} at day 23 and 210 kg CO_2 d^{-1} on day 33 (Fig. 3a). The total injected CO_2 amounted to 4.2 tonnes over the 37-day period.

Four zones with biogeochemically and ecologically similar characteristics were chosen: Zone 1(Z1) was the epicentre of the release; Z2 and Z3 were 25 and 75 m distant from the epicentre respectively; Z4 was the control site at 450 m from the epicentre (Fig. 1). All zones were situated along the 10 m isobath. During the release phase up to 35 (depending on the injection rate and tides) individual bubble streams were observed by scuba divers at the epicentre of the release (Z1) rising from the sediment into the water column above it (https://www.youtube.com/watch?v=N_CUdiI5_r4 and Supplementary material). The control site (Z4) was assumed to be unaffected by the CO_2 release. For further details on the experimental methodology see Taylor et al., 2014 (this volume).

2.2. Instruments and sensors

Instruments' deployment and maintenance at the release site in Ardmucknish Bay during the experiment were undertaken by scuba diving, assuring for precise positioning and handling of the equipment. Boat-deployed water column sampling and profiling (5L Niskin bottle and SBE19 CTD from Seabird Inc.) was done from R/V Soel Mara using the onboard winch.

Tidal information and relevant weather data (solar radiation, wind speed and direction, precipitation and atmospheric pressure) were obtained at an hourly interval

from Poltips software and from the permanently installed weather stations at SAMS, and at nearby Dunstaffnage, respectively. To facilitate the wind pattern analysis, high resolution (2km grid) Atmospheric WRF model was run over West Scotland for the period of CO_2 experiment.

Table 1. Summary of the deployments and instruments used in this study.

Instrument_ deployment	Measuring parameters	Period (dd.mm)	Zone	Phase of experiment	Water depth
Seaguard_D1	pCO_2, O_2, C/T	04.06-12.06	Z1	Release	10-12m
Seaguard_D2	pCO_2, O_2, C/T, currents	12.06 -19.06	Z1	Release	10-12m
Seaguard_D3*	O_2, C/T, currents	19.06 - 22.06	Z4	Release	11-13m
Seaguard_D4	pCO_2, O_2, C/T, currents	22.06 - 29.06	Z1	Release/ Recovery	10-12m
Seaguard_D5	pCO_2, O_2, C/T, currents	05.07 - 13.08	Z1	Recovery	10-12m
Seaguard_D6	pCO_2, O_2, C/T, currents	17.09 -29.10	Z1	Recovery	10-12m
ISFET_D1	pCO_2, T	18.05 - 01.06	Z1	Release	10-12m
ISFET_D2	pCO_2, T	05.06 -25.06	Z1	Release	10-12m
CONTROS_D1	pCO_2, C/T/D	22.06	Z1-Z4	Release	9-14.7 m
CONTROS_D2	pCO_2, C/T/D	27.06	Z1-Z4	Recovery	11-13.6 m
RCM#419_D1	C/T, currents	09.05 -18.06	Z3	Release	11-13m
RCM#419_D2	C/T, current	18.06 - 29.06	Z4	Release/ Recovery	11-13m
RCM#419_D3	C/T, current	29.06 - 18.09	Z4	Recovery	11-13m
RCM#643_D1	C/T, current	09.06 - 18.06	Z4	Release	11-13m
RCM#643_D2	C/T, current	18.06 - 29.06	BI†	Release/ Recovery	25-27m
RCM#643_D3	C/T, current	29.06 - 18.09	BI†	Recovery	25-27m

**pCO_2 sensor's protection cap left on resulting in no data*
† Bay inlet

In the work presented here data collected by four different types of instruments (a-d) was used (see Table 1 for deployment details).

(a) A Seaguard® autonomous datalogger from Aanderaa Data Instruments, www.aanderaa.com, (Fig. 2b) was fitted with a single point Doppler Current Meter (Victoria et al., 2011), a temperature and a conductivity/salinity probe, an oxygen optode (Tengberg et al., 2006) and a new type of pCO_2 optode recently described in Atamanchuk et al. (2014). In short, CO_2 gas diffuses from the surrounding water through a gas-permeable membrane into the sensing layer of the pCO_2 optode, where as a consequence the pH is modified. The magnitude of pH change is correlated to the pCO_2 level outside the membrane. The embedded DLR (Dual Lifetime Referencing) material exhibits a pH dependent fluorescence change, which is detected as a phase shift value of returning red light. Response time (τ_{63}) is between 45 sec (at 40°C) and 4.5 min (at 0°C). Observed precision of the sensors is ±2-3 µatm and absolute accuracy is 2-75 µatm; better accuracy is achievable through *in situ* calibration. Stability of the sensors during long-term deployments was shown to be longer than 7 months (Atamanchuk et al., 2014).

The pCO_2 optode was calibrated before the deployment at 40 points (10 pCO_2 concentrations and 4 temperatures) using a temperature controlled water bath that was bubbled with different gas mixtures. In addition the 3-D calibration plane was adjusted *in situ* using one-point referencing methodology (Atamanchuk et al., 2014) and a reference value from water sample taken on day 14 of the release experiment. This value was assumed to represent the background pCO_2 even though it was taken before the actual measurements of the optode commenced (day 18). Following water samples' data served as a reference for subsequent accuracy control (Fig. 4a, Table 2).

Based on factory specifications the absolute accuracies for data from other sensors presented here were estimated to be: ±1 % for current speed measurements, ±5° for current direction, ±0.05°C for temperature and ±0.05 for salinity. The oxygen optode

was saturation checked against atmospheric values in-between deployments; the absolute accuracy was estimated to be ±3%.

None of the Seaguard® sensors demonstrated detectable drift (within sensor specifications) during the five-months period that the instrument was used in this project, and no major bio-fouling was noticed at the five occasions that the instrument was lifted, cleaned and redeployed.

The Seaguard® instrument was anchored to the bottom by burying the housing halfway into the sediment (Fig. 2b) with the sensors measuring every 15 min ~30 cm above the seabed. The instrument was recovered, inspected for damages, cleaned, its data downloaded and it was subsequently redeployed at five separate occasions (Table 1) during the QICS experiment. Each time the instrument was redeployed, it was placed as close as possible to the same location at the release site (Z1). Gaps in data recorded with the instrument during five months of the project was either due to servicing, when the instrument was taken out of the water for few hours, or because it was used in other projects, i.e. long gap between deployments 4 and 5 (Table 1, Fig. 4). On one deployment (Seaguard_D3, see Table 1), the pCO_2 sensor protection cap was left on by mistake while deployed at Z4, and hence the data were excluded from further analysis.

(b) A cabled on-line ion-sensitive field-effect transistor (ISFET) based (e.g. Shitashima and Kyo, 1998; Shitashima et al., 2002; Martz et al., 2010) pH/pCO_2 sensor (Shitashima et al., 2008; Shitashima et al., 2010) was deployed at the epicentre (Fig. 2b). The ISFET based pH sensor uses an ion-sensitive field-effect transistor as the pH electrode, and a chloride ion selective electrode (Cl-ISE) as the reference electrode. The ISFET is a semiconductor made of p-type silicon coated with SiO_2, with Si_3N_4 as the gate insulator surface that is the ion-sensing layer. In aqueous

media, the interface potential between the reference electrode and the sensing layer is a function of the activity of the H^+ ion, i.e. pH. The Cl-ISE is a pellet made of several metal chlorides having a response to the chloride ion, a major element in seawater. The electric potential of the Cl-ISE is stable in the seawater, since it has no inner electrolyte solution. The devised pH sensor shows quick response time ($\tau_{90} < 1$ s) with high accuracy (± 0.005 pH).

The principle of pCO_2 measurement using ISFET-pH technology is as follows. Both the ISFET-pH electrode and the Cl-ISE of the pH sensor are sealed in a unit with a gas permeable membrane whose inside is filled with inner electrolyte solution with 1.5% of NaCl. The pH sensor can measure changes in pCO_2 from changes in the pH of the inner solution, which is caused by penetration of CO_2 through the membrane. An amorphous Teflon membrane (Teflon AF™) manufactured by DuPont was used as the gas permeable membrane. The *in situ* (3000 m depth, 1.8°C) response time (τ_{90}) for detecting changes in pCO_2 was < 60 seconds (Shitashima et al., 2013). Response time of ISFET sensor at the conditions of this experiment was not estimated.

The pCO_2 sensor data were calibrated *in situ* on day 2 of the gas release and on day 5-6 using baseline values. *In situ* calibration involved correction of an existing laboratory calibration of the pH/pCO_2 sensor (not shown in this paper) and the data (depth, temperature, salinity and A_T) of reference bottom water samples (see *2.3. Discrete water samples*). Since background pCO_2 showed daily oscillation, we determined a linear regression of the raw pCO_2 sensor data vs. calculated baseline pCO_2 data, which was used for correction of all the raw ISFET-pCO_2 data before presenting it here (Shitashima et al., 2013).

(c) A HydroC™–CO_2 sensor from CONTROS Systems and Solutions, GmbH, www.contros.eu (Saderne et al., 2013, Fiedler et al., 2013, Fietzek et al., 2014) was deployed twice for profiling and towed measurements in the water column (Table 1). Data for 2D pCO_2 mapping of the sites Z1 through Z4 was collected during the final day of the gas release (day 36) and 5 days after the gas was switched off (day 41). The sensor was towed behind the vessel at 0.1-0.2 knts ~1 m above the bottom along transect from Z1 to Z4. In between the different zones it was heaved and veered by winch at 0.1 m/s.

The HydroC™ determines the pCO_2 in water at an accuracy of better than ± 1% by NDIR absorption measurements within an internal headspace realized by means of a flat membrane equilibrator (Fietzek et al., 2014). The sensor was factory calibrated in water just before and after the two deployments at an *in situ* temperature of 11°C for a range of 200–1700 µatm (Fietzek et al., 2014). The field data was drift corrected by considering the information from the regular sensor zeroings as well as the pre- and the post-deployment calibration of the sensor. Data was processed as described in Fietzek et al. (2014), with the transformation of the two polynomials being carried out based on sensor runtime. All sensor zeroings and subsequent 5 min flush intervals were removed from the data set for response time determination and correction (Fiedler et al., 2013). The sensor's response times were determined automatically from the recovery of the corrected pCO_2 signals within the flush intervals, neglecting the initial pCO_2 values representing gas mixing artefacts within the internal gas stream (Fiedler et al., 2013). An average response time (τ_{63}) of 84 s with a standard deviation of ± 4.2 s was derived from a total of 6 flush intervals during deployment. Since the sensor only experienced a maximum temperature difference of 1°C between all sensor zeroings and the maximum deployment depth was less than 15 m, both temperature and depth influence on the response time were neglected and a constant

response time was assumed for further processing. Using a numerical inversion algorithm the data was finally corrected for the time-lag influence caused by the sensor's time constant (Miloshevich et al., 2004). Different averaging methods were applied to the data prior to the response time correction depending on whether the correction was used to enhance temporal resolution of events or to minimize noise amplification caused by the processing algorithm.

(d) To obtain more background data on currents, salinity and temperature two RCM9 instruments from Aanderaa Data Instruments, www.aanderaa.com, were also deployed and relocated in the area at several occasions (Table 1).

2.3. Discrete water samples

For values of dissolved inorganic carbon (DIC) and total alkalinity (A_T) in the bottom water a series of discrete samples was collected by boat in 5L Niskin bottles 1 meter above the bottom (Table 2). These samples were analysed for DIC and A_T in the lab using standard techniques. For DIC analysis samples were measured in triplicates with an Apollo SciTech DIC analyzer (AS-C3), which uses a LI-COR CO_2/H_2O (LI-7000) infrared analyser to detect the CO_2 released from the samples after acidification with a 10% H_3PO_4 solution. Standard deviation of DIC measurements was typically 0.05% using this system. Potentiometric titration and subsequent Gran evaluation was used for A_T samples (Dickson et al., 2003). For comparison with *in situ* sensor data, the DIC and A_T data were converted into pCO_2 with an overall uncertainly of ±10 µatm using the CO2SYS software (Lewis and Wallace, 1998) using *in situ* temperature and salinity from SBE19 CTD.

Table 2 Summary of the reference pCO_2 data derived from discrete water samples vs. measured by pCO_2 optode, ISFET-based pCO_2 sensor and HydroC™ at Z1.

Date/Day of experiment	Water samples (µatm)	Optode (µatm)	ISFET (µatm)	HydroC™ (µatm)	Tide	CO_2 release
31/05/12 day 14	369	-	461	-	low	Yes
18/06/12 day 32	362	390	671	-	low	Yes
22/06/12 day 36 (morning)	-	-	846	367† (538,508)	high-low	Yes
22/06/12 day 36 (afternoon)	-	-	807	362† (737, 479, 504)	low-high	Yes
27/06/12 day 41 (morning)	348	397			low-high	No
27/06/12 day 41 (afternoon)	-	377	-	368†	high-low	No
11/07/12 day 55	349	380*	-	-	high	No
18/09/12 day 90	373	342	-	-	low	No

**Data indicates the value measured closest to the time of water sampling for referencing.*
†Data resembles averaged baseline values with the peak values in brackets.

2.4. Multivariate data analysis

Recorded data from the Seaguard® at CO_2 release rate, gas release rates, tidal oscillations and meteorological parameters such as air and water temperature, wind direction and speed, precipitation and atmospheric pressure, was used for multivariate data analysis using SIMCA 13 software (Umetrics AB, www.umetrics.com). First, a Principal Component Analysis (PCA) was applied to each deployment dataset (Seaguard_D1-D2, _D4-D6) to identify dependencies between the variables, such as

pCO_2, oxygen, salinity, temperature, gas release rate (where applicable), tidal conditions and meteorological parameters. PCA usually serves for initial inspection of data for outliers, identifying significance of each factor based on a simple analysis tools (scatter and loadings plots, coefficients list, etc). After comparison of the patterns for the gas release phase and recovery phase, conclusions about the response of the system to external CO_2 supply were made.

Based on the outcome from PCA, a Partial Least Squares (PLS) regression model was used to identify parameters, which contributed significantly to pCO_2 and oxygen variations both during the gas release (Seaguard_D1, _D2, _D4-release) and after it was cut off (Seaguard_D4-recovery, _D5, _D6). A supervised PLS model aimed to put pCO_2 and oxygen variations into a context of their correlation with each other and the relation to other parameters. For this pCO_2 and oxygen parameters were assigned in the model as Y variables or result variables, which depend on X variables, i.e. other measured parameters.

2.5. Hydrodynamic modelling

High resolution unstructured grid hydrodynamic model for Loch Etive and Ardmucknish bay, developed at SAMS (Aleynik et al., 2012), was used for modelling of the hydrodynamic conditions at the site. A major advantage of the Finite Volume Community Ocean Model (FVCOM) used here, is in its geometric flexibility, making it a suitable solution for hydrographical modelling along complex coastlines and bathymetry, such as off the West coast of Scotland. The model consists of 6601 horizontal non-overlapping triangular elements and 3776 vertices, with enhanced horizontal resolution (22 m) in the narrows and over the sills (Connel, Bon Awe). At the CO_2 release site, the model has an effective resolution of 120-180 m. In the

vertical dimension, the model consists of 11 terrain following layers. FVCOM is a primitive-equation, free-surface, hydrostatic model described in details in Chen et al. (2003). A model simulation was performed using real-world data – laterally it was forced with a set of CTD data from fixed platforms deployed around Ardmucknish Bay. Tidal forcing was calculated with 6 major tidal harmonics (M2, S2, N2, K2, O1, K1) for the nearest port in Oban, and the meteo-forcing parameters (short-wave and net heat flux, precipitation/evaporation, atmospheric pressure) have been derived from the Met-Office weather station at Dunstaffnage. Freshwater runoff was compiled using a lagged precipitation rate over the catchment area. The forecast parameters of the model include surface elevation, temperature, salinity, current velocity and with the dye-CO_2 module developed by Torres et al. (2012, pers. communication) prediction of several components of the carbonate system - DIC concentration, pH and pCO_2 in seawater - is also possible (see Supplementary material).

3. **Results**

3.1. pCO_2 during gas release

Figure 3a presents details of pCO_2 changes during the release phase, continuously measured with the two different independent sensors systems, i.e. pCO_2 optode and ISFET-pCO_2, along with the tidal conditions and gas release rates. Correlation between pCO_2 values measured by optode and ISFET-based sensor, and water samples data is given in the Table 2. Figure 3b shows pCO_2 variations measured with optode and ISFET-pCO_2 in correlation with tidal circulation. Figure 3c highlights the redeployment of Seaguard® instrument at the release site and related to this event changes in pCO_2 and oxygen time-series.

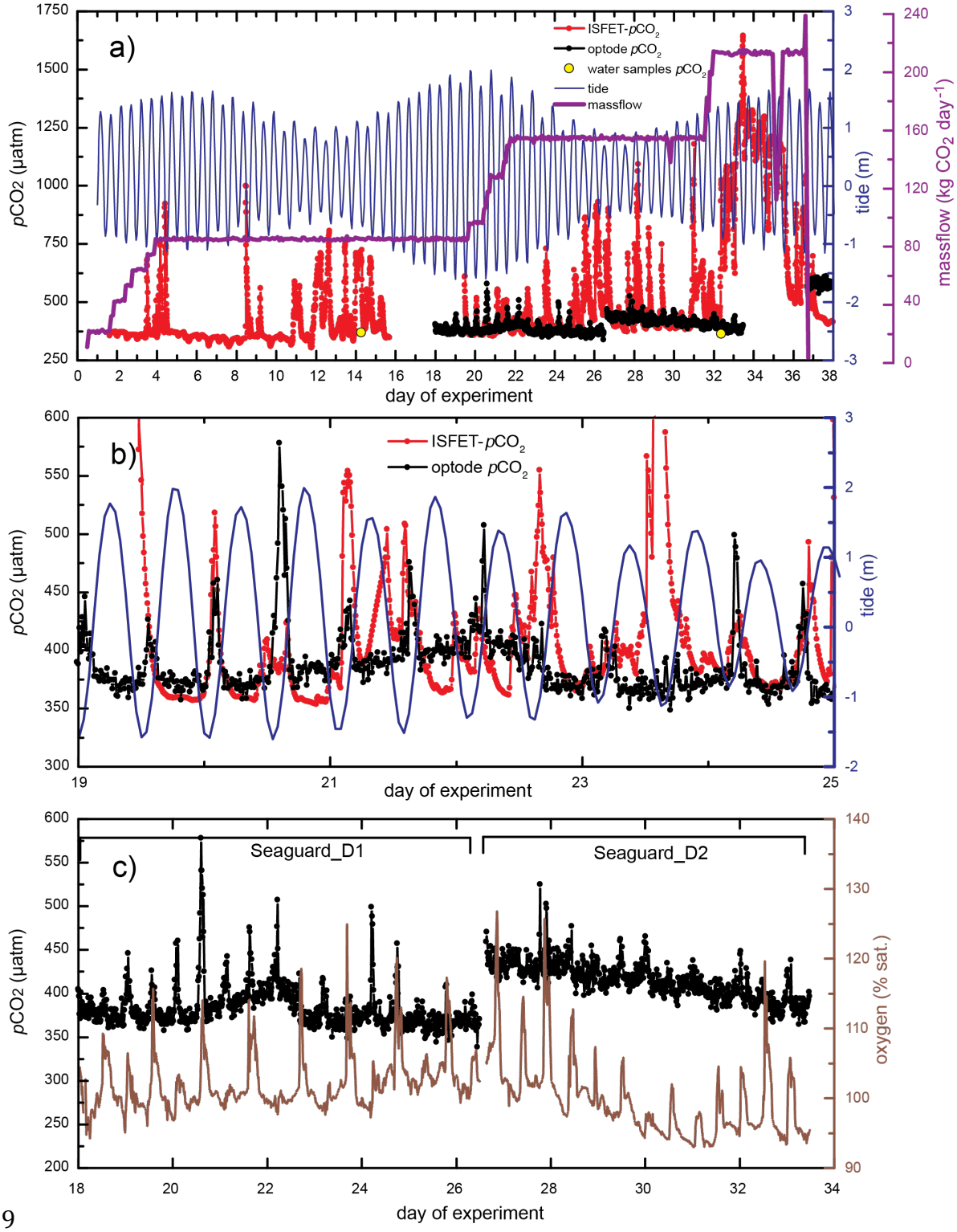

Fig. 3. Summary of data collected during the QICS campaign.
a) period of CO_2 release: pCO_2 data from optode (black line) is compared to ISFET- pCO_2 sensor (red) with respect to tidal variability (blue) and mass flow rate of CO_2 release (violet). Drop in the massflow rate between the days 35 and 36 was due to freezing of the system, which delivered CO_2;
b) correlation between the peaks in pCO_2 optode and ISFET- pCO_2 data and tidal circulation at Z1 during the release;
c) pCO_2 and oxygen time-series recorded during two deployments of the Seaguard® at the release site (Z1). A gap on day 26 indicates recovery and redeployment of the instrument. Spikes on both time-series are attributed to tidal cycles at the site.

A strong dependency between low tide and pCO_2 optode measurements was observed and is highlighted below in *3.4. Multivariate analysis*. A tidal relation was also visible from the ISFET based pH/pCO_2 sensor deployed about 1 meter away from the Seaguard® (Fig. 3b). This sensor was placed ~3 cm above the seafloor, at the rim of one of the pockmark actively venting CO_2. Although having very similar baseline values, e.g. 356±4 µatm for ISFET-pCO_2 sensor and 369±7 µatm for pCO_2 optode during days 18-21 of CO_2 release, the ISFET-pCO_2 sensor showed generally higher amplitude pCO_2 peaks during low tide (up to 420-900 µatm) comparing to the corresponding peaks from the pCO_2 optode (up to 400-580 µatm). Most of the tidally induced pCO_2 peaks from both the optode and ISFET sensors did concur, but not always (Fig. 3b).

The tidal pCO_2 peaks were not reflected at all in the data from discrete water samples collected randomly ~1 m above the seabed just outside the 'footprint' of the bubbling area in Z1. The water samples appeared to reflect approximate baseline levels for pCO_2 at the release and did not represent values of peak concentrations: values showed 362 µatm on day 32, while optode and ISFET- pCO_2 detected 390 and 671 µatm, respectively.

Steep vertical and horizontal pCO_2 gradients were observed while towing the CONTROS HydroC™ sensor ~1 m above the bottom from Z1 to Z4 on day 36, the last day of the gas release. At the Z4 (control site) the sensor measured a pCO_2 of 368±2 µatm without significant spatial heterogeneity. For Z2 and Z3 the same values were obtained, 363±2 µatm, which were of comparable magnitude to those at the control site. When measuring closer to the epicentre in Z1, baseline values at the same depth were 367±1 µatm and 362±2 µatm in the morning and the afternoon, respectively. Sharp pCO_2 peaks of as high as 540 µatm and 740 µatm in the morning and the afternoon respectively, were observed when the sensor was towed through the

area with active venting of CO_2, i.e. within the 'footprint' of the gas release (Fig. 5a shows the afternoon data). At the same time ISFET- pCO_2 recorded 800-850 µatm closer to the bottom. Later during the same day, the pCO_2 optode recorded ~570 µatm pCO_2 30 cm above the seabed and the ISFET pCO_2 sensor showed as high as 1250 µatm at 3 cm above the seabed. The fact that HydroC™ detected higher peak values in the afternoon correlates with the tide dependency observed by the sensors deployed on the seabed. Low tide occurred at the site in conjunction with the afternoon measurements as can be seen in the lower water depth of Fig. 5a compared to Fig. 5b, which shows a transect of the same area obtained during high tide.

At two occasions distinct peaks in the HydroC™ signal even suggest detection of ascending gas bubbles in the water column (one example depicted in Fig. 5a at around 14:32). This observation was underlined by visual evidence of gas bubbles at the water surface around the same time. Moreover, the towed HydroC™ measurements showed distinct pCO_2 differences between the surface water and the bottom water (see Fig. 5b). It could be observed that these differences where influenced by tides and currents as they contributed to mixing of the entire water column within the experimental area, thus affecting the observed gradients (data not shown here).

3.2. pCO_2 during recovery period

ISFET-pCO_2 sensor showed values, which approached the background level, starting already from day 35 (one day before the gas was shut off) and levelled off at ~350 µatm on day 37. Actual release of CO_2 gas was stopped after day 36, which was followed by decline in the pCO_2 concentrations at the epicentre as detected by pCO_2 optode (Fig. 6). Within 7 days after terminating the gas flow, pCO_2 values had reached stable baseline partial pressure of ~345-355 µatm. The post-injection

recovery pattern was also supported by data from discrete water samples (Table 2): DIC and A_T values increased by 75 and 105 µmol kg SW^{-1} and stabilized at the levels of 2095 and 2213 µmol $kgSW^{-1}$, respectively (Fig. 6). As the relative increase in A_T is higher than the increase in DIC, pH shifts to higher values indicating decrease in pCO_2. In Z1 the HydroC™ pCO_2 sensor measured on average 368±2 µatm ~1 m above the bottom on the fifth day of recovery (day 41, Fig. 5b). With measured pCO_2 values of 369±2 µatm, 368±2 µatm and 370±1 µatm for zones Z2, Z3 and Z4 respectively no significant spatial variation was detectable.

After recovery to background values, the partial pressure measured by the pCO_2 optode typically oscillated with ± 30 µatm around mean value of ~360 µatm. However, between August 2nd and 4th pCO_2 levels increased significantly with ~100 µatm compared to background values. A similar event happened during August 8-9th and resulted in an additional rise in pCO_2 with ~70 µatm (Fig. 4a). Both these occasions coincided with distinct changes in the general circulation pattern and in the direction of the water flow, as recorded by the current meters on the Seaguard® and the RCM instruments (see *3.5. Water circulation in Ardmucknish Bay: recorded velocity regime*).

3.3. Background parameters (temperature, salinity, currents and oxygen)

Results from June-October 2012, when the Seaguard® instrument was deployed, are presented in Fig. 4. The clear influence of tides is visible in most of the data. Temperature varied between 9.9-14.3°C and followed the general seasonal pattern with increasing temperatures from May to August and slowly decreasing through September-October to 12.5°C. Depending on tidal conditions temperature changed within ±1°C. Recorded temperature time-series showed negative spikes at low tide

during September-October, and positive spikes during June-August, meaning higher temperature at the surface during summer.

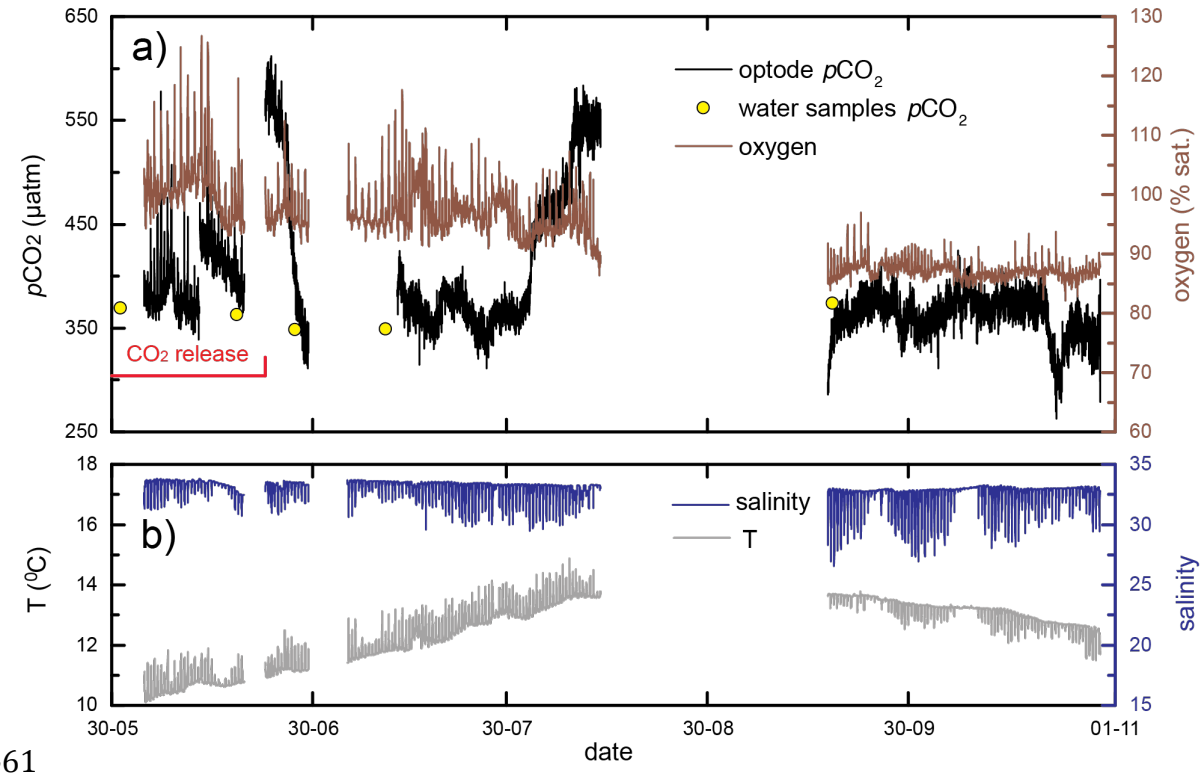

Fig. 4. Summary of Seaguard® data over June-October 2012.
a) pCO_2 and oxygen with a marked period of gas release, and b) temperature and salinity time-series recorded at the release site (Z1). Yellow circles in a) indicate pCO_2 data calculated from water samples analyzed for DIC and A_T. Gaps in the data are due to service of Seaguard® instrument or its' use in a different project.

Salinity varied between 25.7 and 33.8 with tidally induced salinity oscillations in the order of 1-5, and with higher amplitudes during the final September-October deployment. It is worth to notice that water in Ardmucknish Bay was freshening by river discharge, and salinity gradually decreased from 33.4 to 32.5 during June-October (Fig. 4b)

Currents were strongly affected by the tidal circulation. They varied between 0-40.5 cm/s with an overall average of 3.3 cm s^{-1}. The relatively weak average current speed reflects the position of the instrument close to the bottom. The Doppler Current Sensor of the Seaguard® was positioned about 40 cm above the seabed, which is

likely to be close to the logarithmic boundary layer. The two other recording current meters (Table 1) where positioned in frames ~80 cm above the seabed. These instruments recorded somewhat higher average current speeds, 4.8 cm s^{-1} (RCM#643) and 3.6 cm s^{-1} (RCM#419) respectively, from May-September. Measurements from the current meters were used to calibrate and validate the circulation model used in this study.

Oxygen varied between 60-127% air saturation (Fig. 4a) in the bottom water. Especially in the beginning of June a combination of tides and primary production/consumption could lead to 40% changes in air saturation in some hours. There was a general decrease in the average air saturation from ~105% in the beginning of June to ~85% in the end of October.

Oxygen saturation time-series during post-injection period showed moderate daily oscillations correlating with tidal circulation in the bay. The amplitude of these oscillations where higher during June-August, governed by primary production and availability of solar radiation at that period. In September-October the amplitude of oscillations was 2-3 times lower, and mainly controlled by temperature changes at the bottom due to tidal circulation. At that period, surface water was colder than near the bottom, implying lower temperature and higher oxygen concentration at low tide.

3.4. Multivariate analysis

PCA analysis of the collected data showed a poor correlation between weather parameters, such as wind speed and direction, precipitation, PAR and air temperature, and variations in pCO_2, oxygen, salinity, temperature, currents in the bottom water; and tidal activity. Hence weather data was excluded from further evaluation.

A supervised PLS model for each of the five Seaguard® deployments in Z1 (Table 1) showed correlation between the variations of oxygen and pCO_2 in particular, and between the variations of oxygen and pCO_2 and the other measured parameters (salinity, temperature and tides) in general. At the time when the Seaguard® was deployed at the epicentre (Seaguard_D1, _D2, _D4-release) of gas release, a strong correlation between peaks in pCO_2 and low tide was observed, and appeared as equally distanced from origo (centre point) variables in the scatter plot (Fig. 7a). No clear correlation in the pair pCO_2-oxygen was identified when the external source of CO_2 was in operation during gas release.

Multivariate analysis of post-injection deployments (Seaguard_D4-D6), in contrary, revealed a clear negative correlation between pCO_2 and oxygen variations, while connection to the tidal cycle weakened (Fig. 7b).

3.5. Water circulation in Ardmucknish Bay: recorded velocity regime

The dominating circulation pattern at the release site is determined by a combination of coastline, bathymetry, tides and, to a lower extent, by the wind pattern. A jet current heading toward the NW coast of the Ardmucknish bay is formed at each tidal cycle on the ebb stage. When the leading edge of the tidal ’bora’ (a train of internal waves set at the tidal front) reaches shallower water the flow splits into a pair of smaller cyclonic and antic-cyclonic ‘eddies’, which decay when approaching the opposite shore.

The progressive vector diagrams calculated from the velocity records of the three current meters deployed at different distances from the impact site Z1 demonstrate the shift in direction and smaller variations in intensity of the general flow, which confined in time with the relocation of the instruments (Fig. 8a and Table 2). The

changes in the circulation pattern and velocity records also correlated with wind velocities maps at 10m height over Ardmucknish Bay (Supplementary material).

Long-term deployment data from the RCMs and Seaguard® (June 6th-October 28th) confirmed what was found with the short–term record analyses: at Z4 the velocity vector rotation was predominantly counter clockwise (CCW) cyclonic. At both the near source sites Z3 and Z1, the velocity vector rotation was clockwise (CW) anti-cyclonic.

The Seaguard® current profiler registered several occasions with sudden changes in the main flow Between July 5th and July 27th the flow was predominantly towards NE. On July 28th it changed its direction by ~180 degrees towards SW until July 31st. From August 1st to August 12th it changed again towards ENE gradually veering towards E. From the recorded pCO_2 time-series (Fig. 4a) it is seen that the latter change in circulation coincided in time with the two-step elevation in pCO_2 values compared to the baseline.

4. Discussion

4.1. Detection of CO_2 release

The QICS CO_2 release experiment proved to be challenging, but yet feasible in terms of chemically detecting the signal from and describing the distribution of the released CO_2, escaping from the seabed into the overlying water column.

The distribution of gaseous and dissolved CO_2 in the water column was heterogeneous in both time and space during the release with bubble-streams regularly shifting location within the limited 'footprint' of the release (Cevaloglu et al., this issue) and also varying in intensity with the hydrostatic pressure (Fig. 3a, b;

Blackford et al., submitted). The complex hydrodynamic environment typical for coastal- and continental shelf settings made it even more challenging to clearly capture the CO_2 signal of the injected gas.

Using standard techniques, such as ship-based discrete water sampling, made it almost impossible to capture and describe established gradients in pCO_2 due to their lack of temporal coverage and low spatial precision. Thus, it was possible to obtain only background values of pCO_2, which appeared to be insufficiently precise in this case to detect the leakage of CO_2. Discrete water samples were however required to quality assure and *in situ* calibrate the pCO_2 optode and ISFET-pCO_2 sensor. Agreement between optode data and reference values from water samples confirmed stability and reliability of the pCO_2 optode measurements (Fig. 4a), and hence the robustness of this relative new technology.

Continuous *in situ* measurements in contrast to discrete sampling reflected the real dynamics and heterogeneity of pCO_2 distribution as a result of sub-seabed emissions during and after the actual release to the water column. Only 15% of the injected CO_2 escaped the sediment-water interface as gas bubbles at the highest injection rate (210 kg CO_2 d^{-1}); with the remaining 85% still captured within the sediments, either as gas bubbles or dissolved in the porewater (Blackford et al., submitted). The released amounts of CO_2 are a small fraction of what can be expected during real-life acute leaks minding realistic sizes of potential CCS. Nevertheless, the horizons of sharp concentration gradients are detectable by means of high-temporal observations of pCO_2 evolution at different levels above the bottom and different distances from the emission site.

In close vicinity to the pockmarks, i.e. where the gas bubble streams enter the water column, tidally driven oscillations in the pCO_2 had the highest amplitude as detected by the ISFET-pCO_2 sensor. Dissolution of gas bubbles as they ascend in the

water column was described to control distribution of pCO_2 in a vertical plane (Dissanayake et al., 2012; Dewar et al., 2013). Elevated pCO_2 values in the near-bottom masses were further enhanced by mixing of CO_2-saturated pore water, which escapes from pockmarks together with the gas stream. As a result, observed pCO_2 peaks reached up to 1250 µatm at low tide with occasional values of ~1600 µatm. Weak bottom currents and density gradients prevented efficient mixing and restricted upwelling of the denser CO_2 saturated bottom water in favour of horizontal spreading.

At 30 cm above the seafloor, the pCO_2 optode registered peak concentrations of 580 µatm and equal to ± 80-100 µatm pCO_2 horizontal gradient after relocation for ~1m (Fig. 3c). This was interpreted as evidence of strong spatial variability at the release site where the outflowing gas could take different routes through the water column depending on the variable hydrography and/or re-establishing of gas chimneys with a new tidal cycle. After the Seaguard® was moved some of the tidal night-time peaks in oxygen became more distinguished confirming that water column conditions changed after relocation (Fig. 3c).

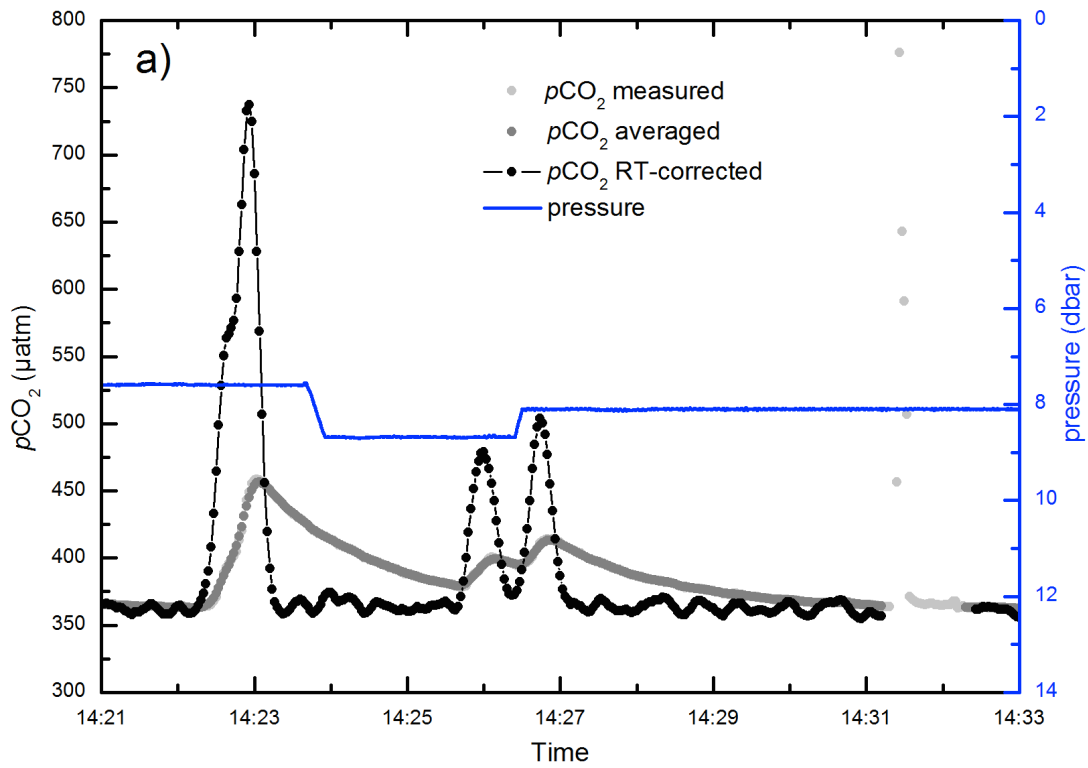

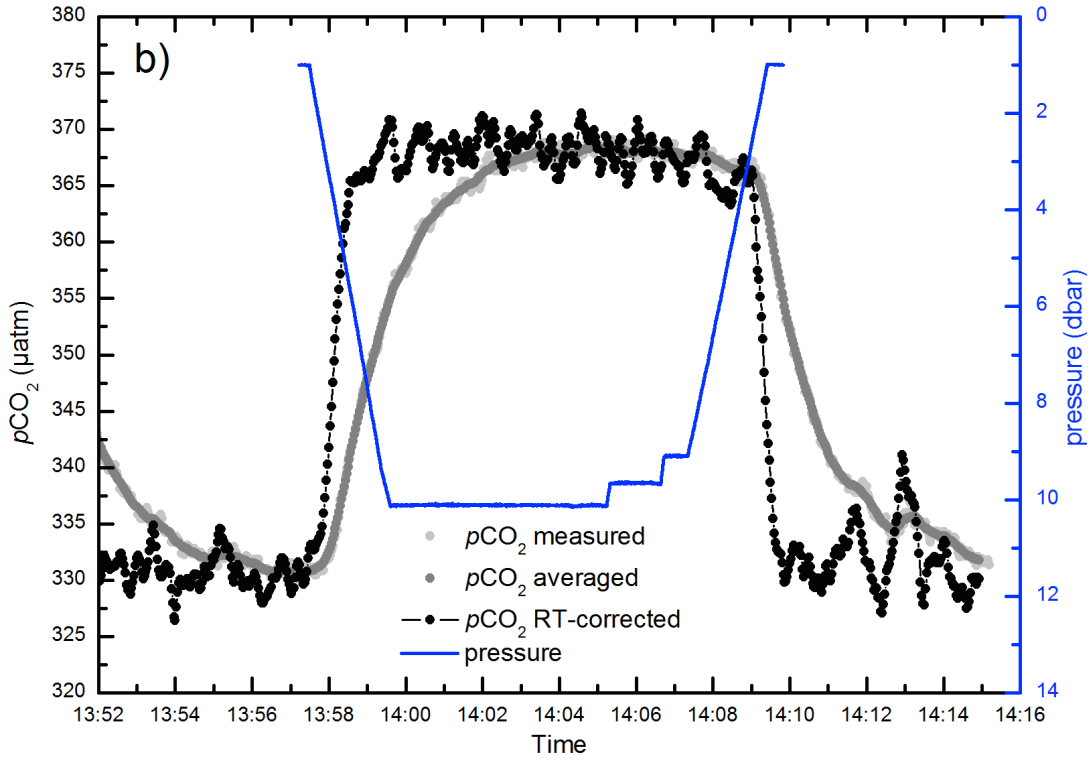

Fig. 5. pCO_2 data obtained from the HydroC™ along with depth information a) while drifting over the release area Z1 on day 36 and b) after the gas release ended on day 41. Note the different scales for pCO_2. In both plots the processed measured pCO_2 signal is shown along with the averaged data (moving average of approx. 12 s width within the upper plot and approx. 30 s within the lower plot respectively) that served as an input to the iterative determination of the response time (RT) corrected pCO_2 time-series.

Occasional pCO_2 peaks with high values in the order of 540-740 µatm, detected during 2D-mapping of the release site with the HydroC™ sensor (Fig. 5a), pointed on the existence of microenvironments around each focused bubble stream, similar to what is observed in a close vicinity to pockmarks. The 'footprint' area of ~30 m in diameter was verified by HydroC™ when drifting over Z1 (Fig. 5a). Since at the given vessel speed of ~0.1 knts a temporal interval of 1 min correlates with a spatial extend of ~3 m, 10 min interval in-between the peaks detected by HydroC™ (Fig. 5a) translates into ~30 m long area of the transect. This indicated dispersion in the water column, which was limited to the restricted area of focused flow of CO_2 bubble plumes, although with slightly shifting position controlled by tidal conditions and hydrography. In this context, high temporal resolution pCO_2 data and response time

correction algorithms as applied within the profiling and drifting measurements of the HydroC™ proved to be useful and powerful observation means. By that distinct pCO_2 peaks on a sub minute time scale with recoveries back to baseline in between could be obtained (Fig. 5a) as well as depth profiles clarified (Fig. 5b).

Increasing flow rates appeared to have minor influence on the baseline values from optode and ISFET-pCO_2 except at the very end when the flow rates were finally increased to 210 kg CO_2 d^{-1}. Intensified CO_2 outflux further enhanced stratification of the water column, resulting into more pronounced difference in baseline values recorded ~3 and ~30 cm above the seafloor, i.e. 1200 and 570 µatm, respectively. In this concern, the values measured ~3 cm above to the bottom seemed to represent microenvironment created by a gas chimney at the pockmark, rather than background pCO_2 value in the water column. The seismic data confirmed that gas chimneys were fully developed all the way up to the sediment-water interface only towards the end of the release phase (Cevatoglu et al., this issue). The higher, but narrower peaks were observed during spring tides and lower, but broader peaks during neap tides. In the latter case the difference in hydrostatic pressure was lower, which allowed pCO_2 peaks to fully develop in-between the tidal changes.

Observations and measurements done in this study are unique in a way that it was a first attempt to assess the impacts of purposefully released CO_2 in the water column by imitating real-life leakages from CCS. A natural analogue of 'failed' CCS, Panarea site, Southern Italy, was well described in terms of the impacts of leaked CO_2 on seawater chemistry (Pearce et al., 2014). The study reports localized effect of seeping gas on seawater pCO_2: natural 350-400 µatm pCO_2 was detected 50 m away from the outflux area, and ~2000 µatm and ~6000 µatm above the epicentre at moderate and high flux rates, respectively. Baseline values in the QICS, however, stayed within the natural range all the time, except for slight elevation to the end of release. This

pointed on a smaller scale of CO_2 release within the QICS. Observed peak concentrations in order of 1600 µatm in this study, are much smaller compared to peak concentrations of 4.5 % CO_2 (or 45 000 µatm) at Panarea site. Higher CO_2 flux rates facilitated much stronger vertical and horizontal gradients of pCO_2 distribution, which could be detected by means of discrete water sampling along a transect at Panarea site. Observations of natural CO_2 leaking sites emphasize the effect of seasonal variability and hydrography both on concentration and distribution of CO_2 gas in the water column (Pearce et al., 2014), which have to be taken into consideration when designing a suitable monitoring strategy for future CCS.

4.2. Recovery after CO_2 release

After the gas was shut off, pCO_2 in the water column recovered relatively fast, within 7 days according to pCO_2 optode. The towed HydroC™ measurements 1 m above the bottom on day 41 did not show any areas of elevated pCO_2 either. A gradual build-up of DIC and A_T in the water column was tracked by simultaneous decrease of pCO_2 levels for ~1 week after the termination of the release, whereafter all three samples seemed to have reached equilibrium (Fig. 6).

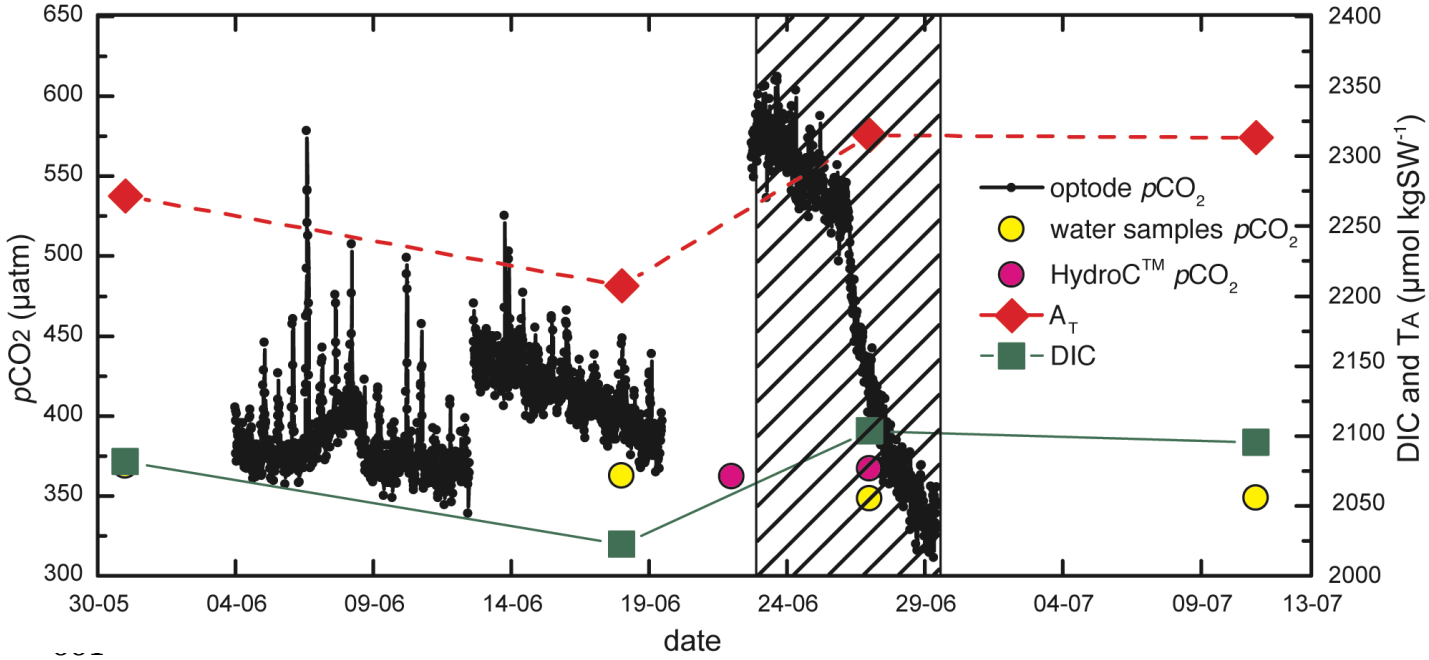

Fig. 6. pCO_2 time-series recorded by optode during the release of CO_2 and until the recovery (shaded area) of the water column. Water samples pCO_2 values derived from DIC/A_T (yellow) and measured by HydroC™ 1m above the bottom (cyan) represent background levels. DIC and A_T analyzed from water samples are plotted for better understanding of recovery pattern shown by pCO_2 optode. Shaded area shows recovery period in the water column.

Observed changes in carbonate chemistry are presumably a combination of natural forcing and flux out of the sediment, where the highest DIC concentrations were measured in the near-surface sediments after the injection was stopped (Blackford et al., submitted; Lichtschlag et al., this issue). Pore water concentrations of DIC and A_T remained high even though the water column data indicated full recovery at day 41. The pore water chemistry (DIC and A_T) returned to background concentrations, most likely through precipitation of $CaCO_3$, three weeks after the termination of the CO_2 release (Blackford et al, submitted).

Data from the ISFET-pCO_2 sensor indicated low values and a fast (<2 days) recovery pattern, which is further discussed in Shitashima et al. (this issue).

4.3. Multivariate data analysis

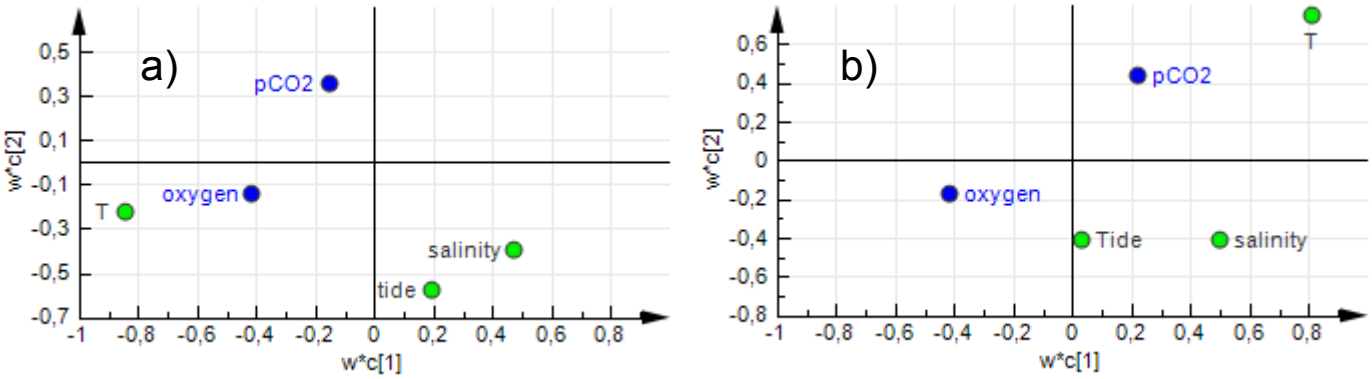

Fig. 7. Graphic representation of PLS model applied in multivariate analysis of the collected data: scatter plot of the Y (pCO_2 and oxygen) and X (T, salinity, tide) weights. Axes represent first (w*c[1]) and second vector component (w*c[2]) of the correlations between the variables. a) Period with CO_2 release. b) Period without CO_2 release. The plots show the relation between Y variables and X variables, and the relation within Y's and X's. Points in the opposite corners and distanced far away from origo (centre point – crossing of the axes) are indicating strong negative correlation between the variables. Points that are closer to the centre have weaker influence to the model.

The multivariate analysis of data turned out to be an efficient tool in distinguishing between periods with and without anthropogenic release. It was shown that in highly dynamic waters like Ardmucknish Bay natural variability is comparable in its levels of pCO_2 variation with the effects of an external CO_2 source (Fig. 4a). Natural forcing, such as biological respiration and exchange of water masses, may be a stronger factor in carbonate system dynamics than the effect of a small acute CO_2 release. We addressed this problem by applying a multivariate analysis technique and looked specifically for the strongest correlation, which dominates in favour to the others. During the CO_2 release phase, the strongest dependence was found between peaks in pCO_2 and low tide – which agreed with the observations of lack of bubble streams during high tide. During the recovery phase, however, multivariate analysis indicated strong negative correlation between the variations of pCO_2 and oxygen, implying that natural factors were now driving the changes in concentrations of these

two gases. The external source of CO_2 was breaking natural correlation between pCO_2 and oxygen.

4.4. Hydrographical conditions

In general, the circulation in Ardmucknish Bay is tidally driven and the influence of tidal circulation was significant on all the measured parameters. In addition the water depth at the release site was ca. 10-12 m, allowing light penetration all the way to the bottom. This led to enhanced oxygen variations due to benthic activity: primary production and super-saturation of oxygen in bottom water during spring/summer days, and respiration during nights, which consumes oxygen (Fig. 4a).

From the observations of pCO_2, main current velocity and velocity vector rotation data, we can conclude that a change in flow direction at Z1 could (a) enhance/inhibit clockwise (CW) anti-cyclonic velocity rotation, and (b) affect water renewal at the site. If the change in flow direction facilitates velocity rotation, this should result in quasi-stationary eddy-like structures, which decay and emerge with every tidal cycle.

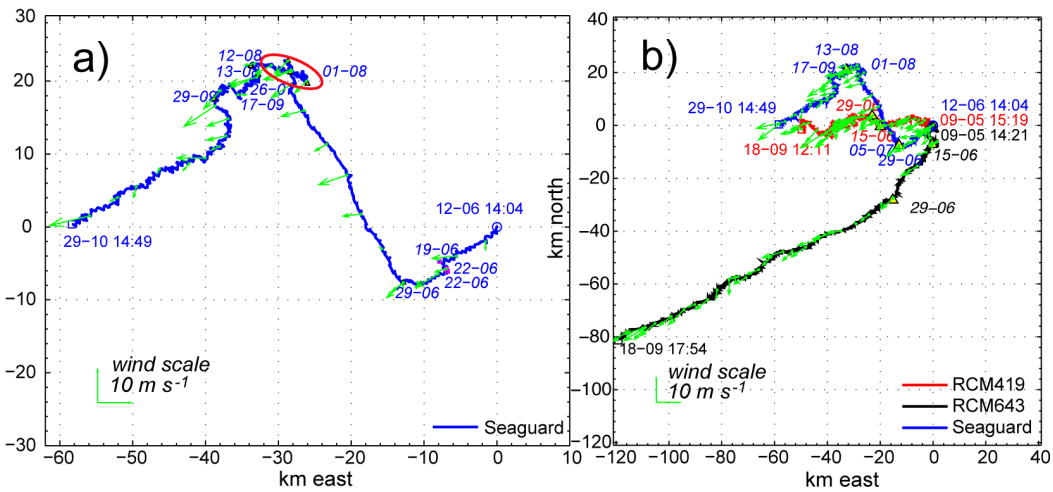

Fig. 8. Predominant water flow direction recorded by the current meters: a) details of Seaguard® data and b) overview of Seaguard® and RCM9 instruments deployed in Ardmucknish Bay in May/June-October 2012. Dates indicate relocation/redeployment of the instrument or change in flow direction. The red oval at a) indicate the change in flow direction between Aug 1st and Aug 12th. Three-daily average wind direction from the Dunstaffnage weather station is indicated with green arrows.

These structures may increase the normal residence time of water and hence accumulate pCO_2 at the site. If the flow direction facilitates renewal of the water with each tidal cycle, this would counteract, in our case, the clockwise anti-cyclonic rotation so that normal eddies lose their velocity, and prevent accumulation of pCO_2. A lowering of the pCO_2 baseline would then be expected. At the release site there were several periods of cyclonic circulation, e.g. in the beginning of August (Fig. 8b), which increased the water residence time, and lead to occasional increases in pCO_2 levels.

5. Conclusions

This work is focused on the technical challenges of detecting anthropogenic CO_2 leakages from a simulated sub-seabed CO_2 storage site using instrumentation installed in the overlying water. Data provided by three different types of pCO_2 sensors in combination with other chemical and physical sensors measuring water column conditions are presented and discussed in this paper.

We showed that purposefully released CO_2 caused tidally-induced pCO_2 oscillations in the water column of Ardmucknish Bay in the order of 30-1250 µatm and resulted in a gradual build-up of the background level from 369 µatm at the beginning up to ~570 µatm close to the seafloor, when the gas flow was the highest, i.e. 220 kg CO_2 d^{-1}. The release caused strong spatial heterogeneity of pCO_2 above the epicentre detected by (a) two sensors measuring within 1 m from each other, i.e. optical pCO_2 and ISFET-pCO_2 sensors, (b) by comparing mentioned devices' data with a 2D horizontal pCO_2 map recorded by a third, NDIR-based pCO_2 sensor, a HydroC™ CO_2, and (c) by relocation of the pCO_2 optode during redeployment. Acidification as a result of CO_2 dissolution in the water column and the sediment was

temporary; the recovery took <7 days and <22 days, respectively, until the system returned to its original natural state.

This study demonstrates that detection of CO_2 leakage from an anthropogenic storage site is possible, but challenging. An aspect of strong heterogeneity of the distribution of the CO_2 gas bubble stream and of the associated dissolved CO_2 species should be taken into consideration as well as a localized 'footprint' of the release. The hydrographically complex system of Ardmucknish Bay introduced an additional challenge bringing more uncertainty to identifying changes associated with CO_2 leakages in contrary to those associated with natural coastal processes. In reality, CCS would most likely be situated at deeper sites with less variable water conditions. One should expect more pronounced effects of CO_2 leaks in the form of an increased background pCO_2 level, though with less pronounced gradients close to the breach. Hence, the detection with permanently deployed sensors measuring pCO_2/pH/O_2 with high sensitivity is suggested as a feasible solution for the targeted areas near the hotspots, such as injection wells, pipelines, and other places of higher risks (e.g. known faults). Depending on the size of the sub-seabed geological storage, a few AUV or towed systems equipped with sensor packages, described in this paper and in Blackford et al. (submitted), should be deployed to scan larger areas on regular intervals. As highlighted in this study, response time of the instruments should be carefully addressed by introducing a correction for signal variation over time. This is applicable for both fixed and movable monitoring platforms. Treatment of incoming data and further assessing the probability of leakage should be done on-line in a framework of multivariate data analysis. This approach decreases risks of misinterpretation of the data caused by e.g. confusing natural variability with an actual leakage.

The results of our study emphasize the necessity of a unique approach in monitoring design of each potential storage site depending on e.g. water depth, bathymetry, etc., and solid knowledge about hydrological and biogeochemical conditions before the storage becomes operational.

6. Acknowledgements

This work was financially supported by SENSEnet (International sensor development network) - a Marie Curie Initial Training Network (ITN) funded by the European Commission Seventh Framework Program under contract number PITN-GA-2009-237868. We thank the UK National Environmental Research Council (NERC), Department of Energy and Climate Change (DECC) and Scottish Government for kindly providing funding to the QICS project (NE/H013911/1). We also acknowledge the Lochnell Estate and Tralee Bay Holiday Park for providing on land site access, the divers at the National Facility of Scientific Diving (NFSD) and the crew on R/V Soel Mara at SAMS for deploying and recovering the instruments. We would like to thank Rachel James and Dough Connelly from the National Oceanography Centre (NOC) in Southampton for seawater sample analysis of DIC and A_T as well as providing background CTD and currents data for the modelling.

7. References

Aleynik D, Stahl H, Inall M. The HYPOX D2.4 Report on Oxygen dynamics in silled basins and its dependence on boundary conditions. 2012. (last accessed on 5th June 2013).

Atamanchuk D, Tengberg A, Thomas PJ, Hovdenes J, Apostolidis A, Huber C, et al. Performance of a lifetime-based optode for measuring partial pressure of carbon dioxide in natural waters. Limnol Oceanogr Methods 2014;12:63-73. [doi: dx.doi.org/10.4319/lom.2014.12.63]

Blackford JC, Jones N, Proctor R, Holt J. Regional scale impacts of distinct CO_2 additions in the North Sea. Mar Pollut Bull 2008;56(8):1461-68. [doi: dx.doi.org/10.1016/j.marpolbul.2008.04.048]

Blackford JC, Stahl H, Bull JM, Berges BJP, Cevatoglu M, Lichtschlag A, et al. Detection and impacts of leakage from sub-seafloor Carbon Dioxide Storage. *Submitted to Nature Climate Change.*

Brewer PG. Direct injection of carbon dioxide into the Oceans. 2003. In: "The Carbon Dioxide Dilemma: Promising Technologies and Policies." National Academies Press, pp. 43-51.

Brewer PG, Peltzer ET, Aya I, Haugan P, Bellerby P, Yamane K, et al. Small scale field study of an ocean CO_2 plume. J Oceanogr 2004;60:751-58. [doi: dx.doi.org/10.1007/s10872-004-5767-9]

Cevatoglu M, Bull JM, Vardy ME, Gernon TM, Wright IC, Long D. First controlled sub-seabed CO_2 release experiment in Ardmucknish Bay, Oban: Insights into gas migration pathways from seismic reflection data and impacts on sediment physical properties. *This issue.*

Chen C, Liu H, Beardsley RC. An unstructured grid, finite-volume, three dimensional, primitive equations ocean model: application to coastal ocean and estuaries. J Atmos Oceanic Technol 2003;20:159–86. [doi: dx.doi.org/10.1175/1520-0426(2003)020<0159:AUGFVT>2.0.CO;2]

Dewar M, Wei W, McNeil D, Chen B. Small-scale modelling of the physiochemical impacts of CO_2 leaked from sub-seabed reservoirs or pipelines within the North Sea and surrounding waters. Mar Pollut Bull 2013;73(2):504-15. [doi: dx.doi.org/10.1016/j.marpolbul.2013.03.005]

Dickson AG, Afghan JD, Anderson GC. Reference materials for oceanic CO_2 analysis: a method for the certification of total alkalinity. Mar Chem 2003;80:185–97. [doi: dx.doi.org/10.1016/S0304-4203(02)00133-0]

Dissanayake A, DeGraff JA, Yapa PD, Nakata K, Ishihara Y, Yabe I. Modelling the impact of CO_2 releases in Kagoshima Bay, Japan. J Hydro-Environ Res 2012;6(3):195-208. [doi: dx.doi.org/10.1016/j.jher.2012.02.001]

Fiedler B, Fietzek P, Vieira N, Silva P, Bittig HC, Körtzinger A. In situ CO_2 and O_2 measurements on a profiling float. J Atmos Oceanic Technol 2013;30:112–26. [doi: dx.doi.org/10.1175/JTECH-D-12-00043.1]

Fietzek P, Fiedler B, Steinhoff T, Körtzinger A. In situ quality assessment of a novel underwater pCO_2 sensor based on membrane equilibration and NDIR spectrometry. J Atmos Oceanic Technol 2014; *31*(1):181–96. [doi:dx.doi.org/10.1175/JTECH-D-13-00083.1]

Gough C and Shackley S (eds) 2005. An Integrated Assessment of Carbon Dioxide Capture and Storage in the UK, Tyndall Centre Tech. Rpt. 47 http://www.tyndall.ac.uk/sites/default/files/t2_21.pdf

Haszeldine RS. Carbon Capture and Storage: How Green Can Black Be? Science 2009;325(5948):1647-52. [doi:dx.doi.org/10.1126/science.1172246]

Jeong S, Sato T, Chen B, Tabeta S. Numerical simulation on multi-scale diffusion of CO_2 injected in the deep ocean in a practical scenario. Int J Greenh Gas Con 2010;4(1):64-72. [doi:dx.doi.org/ 10.1016/j.ijggc.2009.09.021]

Kano Y, Sato T, Kita J, Hirabayashi S, Tabeta S. Model prediction on the rise of pCO_2 in uniform flows by leakage of CO_2 purposefully stored under the seabed. Int J Greenh Gas Con 2009;3(5):9. [doi:dx.doi.org/10.1016/j.ijggc.2009.03.004]

Kano Y, Sato T, Kita J, Hirabayashi S, Tabeta S. Multi-scale modelling of CO_2 dispersion leaked from seafloor off the Japanese coast. Mar Pollut Bull 2010;60(2):215-24. [doi:dx.doi.org/10.1016/j.marpolbul.2009.09.024]

Kirkwood W, Graves D, Conway M, Pargett D, Scholfield J, Walz P, et al. Engineering development of the Free Ocean CO_2 Enrichment (FOCE) Experiment. MTS/IEEE Oceans 2005:MTS/IEEE #050304-93. [doi:dx.doi.org/10.1109/OCEANS.2005.1640013]

Kirkwood W, Peltzer ET, Walz P, Brewer P. Cabled observatory technology for ocean acidification research. Ocean 2009 – EUROPE 2009;1(6):11-4. [doi:dx.doi.org/10.1109/OCEANSE.2009.5278337]

Lewis E, Wallace DWR. Program developed for CO_2 system calculations. ORNL/CDIAC-105. Oak Ridge (TN): Carbon Dioxide Information Analysis Center, Oak Ridge National Laboratory, U.S. Department of Energy; 1998.

Lichtschlag A, James RH, Stahl H, Connelly D. Effect of a controlled sub-seabedrelease of CO_2 on the biogeochemistry of shallow marine sediments, their porewaters, and the overlying water column. *This issue.*

Martz TR, Connery JG, Johnson KS. Testing the Honeywell Durafet® for seawater pH applications. Limnol Oceanogr Methods 2010;8:172-84. [doi:dx.doi.org/10.4319/lom.2010.8.172]

Miloshevich LM, Paukkunen A, Vömel H, Oltmans SJ. Development and validation of a time-lag correction for vaisala radiosonde humidity measurements. J Atmos Oceanic Technol 2004;21(9):1305–27. [doi:dx.doi.org/10.1175/1520-0426(2004)021<1305:DAVOAT>2.0.CO;2]

Pearce J, Blackford J, Beaubien S, Foekema E, Gemeni V, Gwosdz S, et al. A Guide to potential impacts of leakage from CO_2 storage. British Geological Survey, RISCS 2014.

Saderne V, Fietzek P, Herman PMJ. Extreme variations of pCO_2 and pH in a macrophyte meadow of the Baltic Sea in summer: evidence of the effect of photosynthesis and local upwelling. PLoS ONE 2013;8(4):e62689. [doi:dx.doi.org/10.1371/journal.pone.0062689]

Shitashima K, Kyo M. Application of chemical sensor to oceanography –development of deep sea pH sensor using ISFET. (in Japanese with English abstract). Chikyukagaku (Geochemistry) 1998;15:1-11.

Shitashima K, Kyo M, Koike Y, Henmi H. Development of in-situ pH sensor using ISFET. Proceedings of the 2002 International Symposium on Underwater Technology 2002 ;IEEE/02EX556:106-8. [doi:dx.doi.org/10.1109/UT.2002.1002403]

Shitashima K, Maeda Y, Koike Y, Ohsumi T. Natural analogue of the rise and dissolution of liquid CO_2 in the ocean. Int J Greenh Gas Con 2008;2(1):95-104. [doi:dx.doi.org/10.1016/S1750-5836(07)00092-8]

Shitashima K. Evolution of Compact Electrochemical In-situ pH-pCO_2 Sensor using ISFET-pH Electrode. MTS/IEEE Seattle, OCEANS 2010;1(4):20-3. [doi:dx.doi.org/10.1109/OCEANS.2010.5663782]

Shitashima K, Maeda Y, Ohsumi T. Development of detection and monitoring techniques of CO_2 leakage from seafloor in sub-seabed CO_2 storage. Appl Geochem, 2013;30:114-24. [doi:dx.doi.org/10.1016/j.apgeochem.2012.08.001]

Shitashima et al., *this issue.*

Taylor P, Stahl H, Blackford J, Vardy ME, Bull JM, Akhurst M, et al. Introduction to a novel in situ sub-seabed CO_2 release experiment for quantifying and monitoring potential ecosystem impacts from geological carbon storage. *This issue.*

Tengberg A, Hovdenes J, Andersson JH, Brocandel O, Diaz R, Hebert D, et al. Evaluation of a lifetime based optode to measure oxygen in aquatic systems. Limnol Oceanogr Methods 2006;4: 7-17. [doi:dx.doi.org/10.4319/lom.2006.4.7]

Victoria I. Measuring currents in demanding environments with a SeaGuard® RCM. Current meter conference. Proceedings of the 10th Conference on Current, Wave and Turbulence Measurements (CWTM) 2011:237-45. [doi:dx.doi.org/10.1109/CWTM.2011.5759558]

Walz PM, Kirkwood WJ, Peltzer ET, Hester KC, Brewer PG. Creating controlled CO_2 perturbation experiments on the seafloor — Development of FOCE techniques. Oceans 2008 - MTS/IEEE Kobe Techno-Ocean 2008;1–3:750–3. [doi:dx.doi.org/10.1109/OCEANSKOBE.2008.4531025]

Wilkinson M, Haszeldine RS, Mackay E, Smith K, Sargeant S. A new stratigraphic trap for CO_2 in the UK North Sea: Appraisal using legacy information, Int J Greenh Gas Con 2013;12:310-22. [doi:dx.doi.org/10.1016/j.ijggc.2012.09.013]

8. Supplementary material

Video1 - Introduction to quantifying and monitoring potential ecosystem impacts of geological carbon storage.mp4

Video2 - QICS experiment-replicated CO_2 leak from a CCS sub-seabed storage site.mp4

Model output 1 – An example of modelled tidally driven near-bottom DIC/TCO_2 (µmol $kgSW^{-1}$) distribution with one-hour intervals for the end of May 2012 during the release in Ardmucknish Bay. Black arrows show vertically averaged (barotropic) current velocity in conditional units.

Model output 2 – High-resolution (2km grid) Atmospheric WRF model over West Scotland for the period of the QICS experiment. The picture sequence show be-weekly averaged wind velocity maps at 10 m height, extracted for the centre of the nested domain. Dates above the graph indicate the centre of 2 weeks average period.